

## Relaxation dynamics and transformation kinetics of deeply supercooled water: Temperature, pressure, doping, and proton/deuteron isotope effects

Sonja Lemke, Philip H. Handle, Lucie J. Plaga, Josef N. Stern, Markus Seidl, Violeta Fuentes-Landete, Katrin Amann-Winkel, Karsten W. Köster, Catalin Gainaru, Thomas Loerting, and Roland Böhmer

Citation: *The Journal of Chemical Physics* **147**, 034506 (2017); doi: 10.1063/1.4993790

View online: <http://dx.doi.org/10.1063/1.4993790>

View Table of Contents: <http://aip.scitation.org/toc/jcp/147/3>

Published by the [American Institute of Physics](#)

---

---



**COMPLETELY  
REDESIGNED!**

*Physics Today* Buyer's Guide  
Search with a purpose.

# Relaxation dynamics and transformation kinetics of deeply supercooled water: Temperature, pressure, doping, and proton/deuteron isotope effects

Sonja Lemke,<sup>1</sup> Philip H. Handle,<sup>2,3</sup> Lucie J. Plaga,<sup>1</sup> Josef N. Stern,<sup>2</sup> Markus Seidl,<sup>2</sup> Violeta Fuentes-Landete,<sup>2</sup> Katrin Amann-Winkel,<sup>2,4</sup> Karsten W. Köster,<sup>1</sup> Catalin Gainaru,<sup>1</sup> Thomas Loerting,<sup>2</sup> and Roland Böhmer<sup>1</sup>

<sup>1</sup>Fakultät Physik, Technische Universität Dortmund, D-44221 Dortmund, Germany

<sup>2</sup>Institute of Physical Chemistry, University of Innsbruck, A-6020 Innsbruck, Austria

<sup>3</sup>Department of Physics, Sapienza Università di Roma, I-00185 Rome, Italy

<sup>4</sup>Department of Physics, Stockholm University, SE-106 91 Stockholm, Sweden

(Received 3 May 2017; accepted 23 June 2017; published online 20 July 2017)

Above its glass transition, the equilibrated high-density amorphous ice (HDA) transforms to the low-density pendant (LDA). The temperature dependence of the transformation is monitored at ambient pressure using dielectric spectroscopy and at elevated pressures using dilatometry. It is found that near the glass transition temperature of deuterated samples, the transformation kinetics is 300 times slower than the structural relaxation, while for protonated samples, the time scale separation is at least 30 000 and insensitive to doping. The kinetics of the HDA to LDA transformation lacks a proton/deuteron isotope effect, revealing that this process is dominated by the restructuring of the oxygen network. The x-ray diffraction experiments performed on samples at intermediate transition stages reflect a linear combination of the LDA and HDA patterns implying a macroscopic phase separation, instead of a local intermixing of the two amorphous states. *Published by AIP Publishing.* [<http://dx.doi.org/10.1063/1.4993790>]

## I. INTRODUCTION

Amorphous ices may be viewed as immobilized liquids in which mobility emerges upon heating so that arguably they turn into ultraviscous liquids. The existence of more than one distinct form of amorphous ice<sup>1</sup> has given rise to the concept of polyamorphism,<sup>2,3</sup> which has fueled the notion of the existence of more than one H<sub>2</sub>O liquid.<sup>4</sup> Specifically, a link of high-density (HDA) and low-density amorphous ices (LDA) to the existence of high-density and low-density ultraviscous water has been suggested. The existence of two liquids in the one-component system H<sub>2</sub>O is highly controversial, though, for a recent review, see Ref. 5. The ability to switch reversibly from high-density to low-density amorphous ices by cycling at high pressures has been considered as evidence for polyamorphism.<sup>6–9</sup>

Amorphous ices are metastable with respect to crystalline ices or other amorphous ices, and so the transformation to more stable forms competes with structural equilibration of the amorphous state itself.<sup>10</sup> An ultraviscous liquid can only emerge from amorphous ices if the time scale of microscopic relaxation is much shorter than the time scale of transformation, i.e., if there is a separation of equilibration versus transformation time scales. If, on the other hand, transformation is faster than equilibration, amorphous ices can only be regarded as transient, instable species rather than as metastable ones. This question of time scale separation has not received much attention in the literature, causing some confusion regarding the question whether

distinct liquids as well as a first-order liquid-liquid transition in the one-component system H<sub>2</sub>O are generally possible or not.<sup>11</sup>

The present work reports on dielectric and also dilatometric experiments performed near the glass transitions of amorphous ices. Previously, mostly the dielectric response of low-density forms of amorphous H<sub>2</sub>O was studied,<sup>12,13</sup> and fewer investigations were devoted to the dielectric response of its high-density forms at ambient<sup>14</sup> and elevated<sup>15,16</sup> pressures.

The two variants of high-density amorphous ice that are of interest in the current context are called expanded<sup>17</sup> or equilibrated<sup>18</sup> HDA (eHDA) and unannealed HDA (uHDA). The latter can be prepared by compressing hexagonal ice at 77 K.<sup>17,19</sup> It was shown that uHDA contains “remnants of distorted hexagonal ice”<sup>20</sup> or “nanocrystalline ice I<sub>h</sub> domains.”<sup>21,22</sup> That is, at the nanoscale, the amorphization process is incomplete, which causes reduced thermal stability and an enhanced crystal growth. By contrast, eHDA is prepared from very high-density amorphous ices<sup>23</sup> by decompression at 140 K.<sup>24</sup> Here, higher temperatures and higher pressures are involved in the preparation process, resulting in essentially complete amorphization and much higher thermal stability.<sup>17,18,21,22,25</sup>

In the present work, we access the time scales of relaxation and transformation in eHDA and in LDA emerging thereof, based on the dielectric experiments at ambient pressure and volumetric experiments at high-pressure conditions. Earlier ambient-pressure studies dealing with the transformation from

uHDA to LDA applied time dependent neutron scattering.<sup>26–28</sup> Also some preliminary dielectric data for the transformation from eHDA to LDA were published.<sup>5</sup> None of these studies treated specifically the separation of time scales. It is one of the goals of this work to access it and to investigate several conditions that may impact on the separation of transformation and relaxation time scales, such as temperature, pressure, doping of the amorphous matrix, and proton/deuteron isotope substitution.

We also check whether eHDA shows an isotope effect which is of a similarly large magnitude than the one revealed earlier for LDA<sup>29</sup> as well as for amorphous solid water (ASW).<sup>13</sup> Furthermore, we monitor how an H/D exchange affects the kinetics of the isothermal transformation from the high-density to the low-density amorphous state.

One of the main findings of the present work is that at ambient pressure, the separation of time scales between the dielectric relaxation and the polyamorphic eHDA to LDA transition is at least 2–3 orders of magnitude, even at temperatures somewhat above the glass transition. Similar observations are made for the crystallization transformation of LDA to cubic ice (more specifically, stacking-disordered ice I).<sup>30,31</sup> In particular, our experiments imply that the structural relaxation of eHDA is fast on the time set by the much slower transformation to LDA. Thus, on a phenomenological basis, eHDA can be considered as a sufficiently (meta-) stable state of water and the same is true for LDA.

## II. EXPERIMENTAL DETAILS

The temperature at which the polyamorphic HDA to LDA transition takes place (and hence the related transformation kinetics) is strongly affected by the way the amorphous ices are prepared.<sup>17,18</sup> Calorimetry at ambient pressure<sup>18,32</sup> and crystallization studies at higher pressure<sup>21,22</sup> indicate that the samples most resistant to transformation are eHDA and LDA obtained from eHDA<sup>33</sup> (rather than from uHDA). Thus, here we employ eHDA samples to enhance the separation of time scales. For simplicity, in the following we will usually call the studied ices HDA and LDA.

As described earlier, HDA and LDA samples were prepared by decompressing very high density amorphous ice in a piston-cylinder setup at 140 K to 0.1 GPa for HDA and at ambient pressure for LDA.<sup>24</sup> Deuterated HDA and LDA were prepared by decompression at 143 K. The cylindrical samples with a diameter of 8 mm were then quench-recovered to 77 K and ambient pressure, removed from the pressure cell under liquid nitrogen, and transferred from Innsbruck to Dortmund to carry out dielectric experiments. For the volumetric studies, the quench-recovered HDA samples were left in the pressure cell and transformed to LDA at 1 to 4 MPa by heating at 2 or 3 K/min.<sup>34,35</sup>

Dielectric spectra were recorded in a frequency range from  $10^{-2}$  Hz to  $10^4$  Hz using a Novocontrol system including an Alpha impedance analyzer and a Quatro temperature controller. The samples were finely powdered and transferred to an invar/sapphire cell at liquid nitrogen temperature as previously described.<sup>14</sup> Due to uncertainties regarding the filling

factor of the cell, the dielectric results are presented in arbitrary units. Prior to the acquisition of frequency dependent spectra, temperatures were equilibrated for about 20 min to achieve a stability level of  $\pm 0.1$  K.

## III. EXPERIMENTAL RESULTS

### A. Ambient-pressure dielectric spectroscopy

With the goal to study the time dependent high- to low-density transformation of samples produced from protonated and from deuterated water, it is appropriate to first present their temperature dependent dielectric response. In Fig. 1(a), we show the dielectric loss obtained for deuterated HDA while heating the specimen in steps corresponding to an effective rate of about 0.1 K/min from 110 K to temperatures of 127 K. One recognizes how this slow heating shifts the overall loss patterns to higher frequencies, marking a successive speed-up of the water dynamics. Based on its calorimetric signature, the unfreezing of this dynamics might be called the structural relaxation.<sup>14</sup> Although loss peaks are not fully resolved in the experimental window, comparison with previous data<sup>14</sup> on protonated HDA that are reproduced in Fig. 1(b), reveals a significant isotope effect. Referring to the spectra acquired at 124 K which are emphasized in both frames, one recognizes a deuteration induced slow-down of the dynamics by at least a factor of 20, which is even larger than that previously reported for LDA.<sup>29</sup>

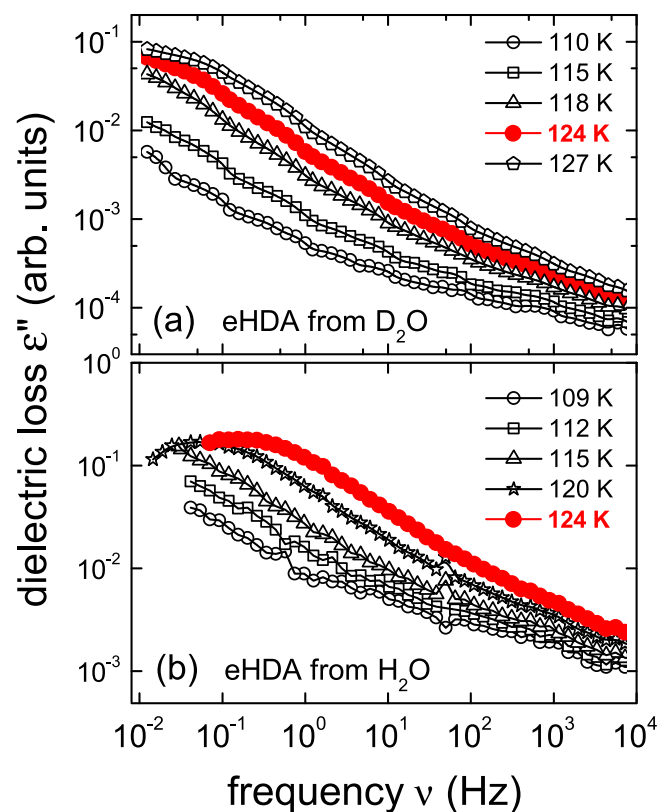


FIG. 1. Comparison of the dielectric loss spectra of (a) deuterated and (b) protonated<sup>14</sup> HDA. In both frames, the data recorded at 124 K are marked in order to highlight that the isotope substitution slows the dynamics in the D<sub>2</sub>O sample by more than a factor of 20.

The transformation kinetics from the high- to the low-density state was studied by isothermal measurements at different temperatures in the 117–123 K range. For each experiment, a different sample (from the same H<sub>2</sub>O or D<sub>2</sub>O batch) was used. After temperature stabilization, the samples were isothermally kept (within  $\pm 0.1$  K) for several hours, in one case up to times of  $5 \times 10^5$  s (more than 5 days). Figures 2(a) and 2(b) show a few examples of those spectra measured at 121 K for deuterated and protonated samples, respectively. During each experiment, dielectric loss spectra were continuously recorded. The time designated “0” in Fig. 2 is defined as the instant at which the first data point (corresponding to the highest frequency of the upper spectrum) is recorded. One recognizes how the overall signal amplitude decreases as the waiting time progresses.

Furthermore, one notes that the shape of the high-frequency flank changes in the course of the transformation. For HDA, cf. Fig. 1 or the spectra shown in Fig. 2 for the shortest waiting times, an excess wing occurs, similar to the observations made for many other glass forming liquids. After the transformation to LDA has occurred, i.e., for the longest waiting times the spectra displayed in Fig. 2 have developed a “bump” for frequencies of a few hundred Hz. This feature was discussed in Ref. 14 for protonated LDA in connection with a possible secondary relaxation that was noted earlier.<sup>36</sup>

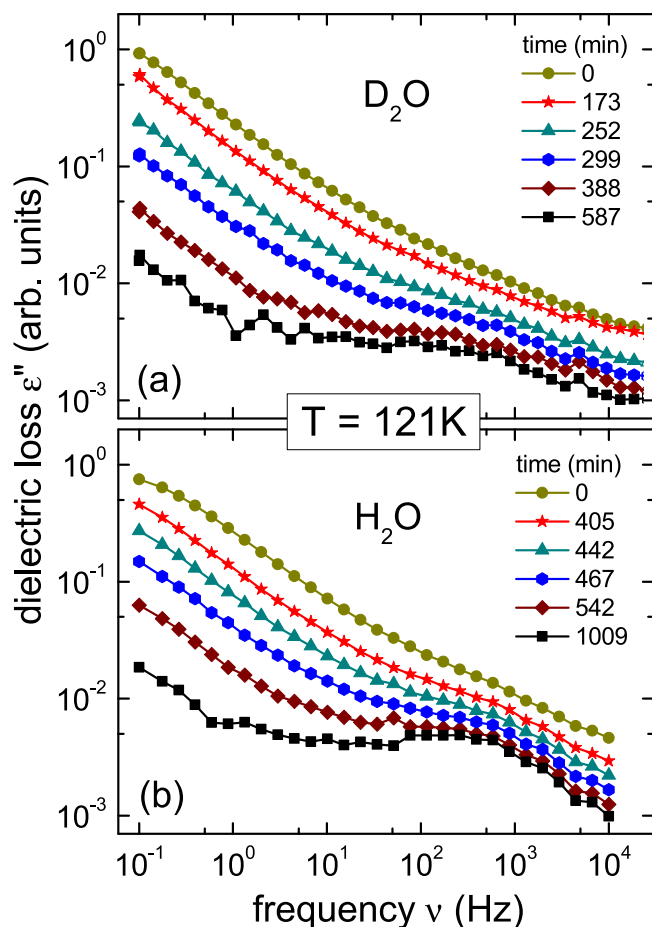


FIG. 2. Dielectric loss curves recorded at 121 K for (a) deuterated and (b) protonated eHDA samples after having annealed them for the specified waiting times  $t$ . The loss of signal amplitude reflects the transformation from the high- to the low-density state of water.

This finding, which certainly deserves further scrutiny, appears similarly also for deuterated LDA. Likewise the excess wing behavior seen for HDA does not depend much on whether the sample is protonated or deuterated.

Generally, under isothermal conditions, a successive loss of signal such as visible in Figs. 2(a) and 2(b) can arise (i) if a loss peak shifts towards low frequencies or/and (ii) if its amplitude decreases. The latter scenario typically applies when the underlying transformation produces a sample devoid of dielectric loss and the decrease of  $\varepsilon''(t)$  directly reflects the decrease of the volume fraction of the starting material. In the present situation, one ends up with LDA, as was demonstrated previously for the protonated variant,<sup>5,14</sup> a material featuring significant dielectric loss. This means that at any given time,  $\varepsilon''(t)$  should be larger than that expected for a transition to loss-free material and its temporal variation provides one only with an approximate measure for the non-transformed volume fraction. This has to be kept in mind for subsequent interpretations.

Waiting time dependent peak shifts and thus scenario (i) can typically be observed in studies of physical aging<sup>37,38</sup> in which temperature down-jumps lead to loss features evolving toward lower frequencies. However, this scenario is incompatible with the present temperature protocol. Conversely, temperature up-jumps would lead to shifts evolving toward higher frequencies, a situation which is also not implied by the present data. This observation taken together with the finding that the transformation times are orders of magnitude longer than structural relaxation times demonstrates clearly that physical aging is not at the origin of the spectral evolution displayed in Fig. 2.

Another possibility for a type (i) scenario would occur if during the conversion HDA and LDA formed a homogeneous mixture with a single relaxation peak shifting in time between the two limits corresponding to neat HDA and neat LDA, respectively. This scenario can be ruled out, since double-peaked neutron<sup>39</sup> and x-ray diffraction<sup>18</sup> patterns were recorded in the past, indicating a two-phase HDA/LDA mixture rather than a homogeneous mixture, at least for isothermal transitions observed in the GPa pressure range. Here, we show that the same also applies for the isobaric transition of HDA to LDA, see Sec. III B. A clear distinction of the various scenarios based on dielectric experiments alone would require tracing the time progression of the dielectric loss peak which is expected to show up at frequencies considerably lower than those shown in Fig. 2.

At present, we are not dealing with physical aging so that such an interference of time scales is not necessarily unavoidable. Nevertheless, for simplicity, we focus on monitoring the time dependent decrease of the loss amplitude. Since the effects are most pronounced at the lowest frequencies, Fig. 3 presents the time evolution,  $\varepsilon''(t)$ , recorded at 0.1 Hz. In some cases, data taken at 1 kHz are included as well, which demonstrates that losses recorded at different measuring frequencies display the same time dependence. Figure 3(a) contains results for a deuterated sample and Fig. 3(b) for a protonated sample. The loss data are all scaled to decay from 1 at  $10^3$  s to 0 at long times. One should be aware that in our experiments the short-time limit is set by the condition that measurements

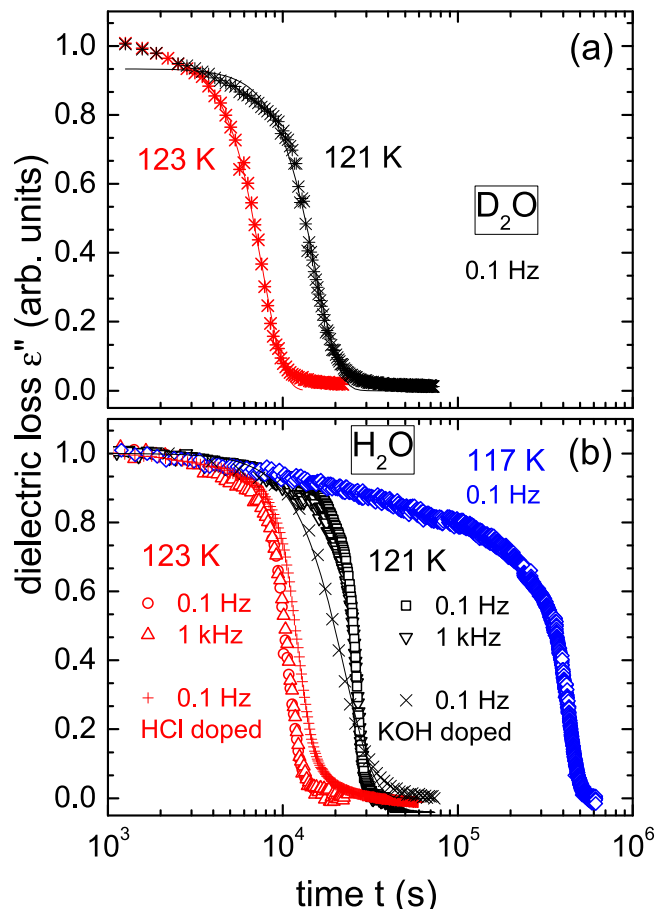


FIG. 3. Time dependent dielectric loss of initially highly dense amorphous samples as recorded at the specified frequencies and temperatures. The curves are scaled to decay from 1 at  $10^3$  s to 0 at long times. Data measured for  $\text{H}_2\text{O}$  ice at 123 K and 0.1 Hz were previously shown in Ref. 5. The lines are fits using Eq. (1) and serve as guides to the eye.

should reasonably start only *after* the temperature is well stabilized.

Inspection of the  $\varepsilon''(t)$  curves collected in Fig. 3 creates the impression that two time regimes should be discerned. At relatively short times which could mark an induction period for the transformation, a steady but less pronounced decrease of the loss amplitude occurs. Then, Fig. 3 shows that at later times a precipitous loss of the dielectric signal follows. A related two-regime behavior is also evident from waiting time dependent neutron data.<sup>27,28</sup>

It is instructive to monitor the transition of LDA to cubic ice, and we have done so for several of the specimens for which transformation data were reported above. As an example, the inset of Fig. 4 displays the dielectric loss spectra of HCl-doped protonated LDA acquired at 143 K while the crystallization to the cubic phase is progressing. Undoped cubic ice is known to display very slow dynamics<sup>40,41</sup> and thus it exhibits little dielectric loss when extrapolated to 143 K. This is reflected by the decrease of  $\varepsilon''(t)$  that we observe during crystallization of the undoped material, see Fig. 4. When investigating HCl doped LDA at 143 K, after the induction period, one observes not a decrease but an increase of the overall loss (see inset of Fig. 4) and implicitly of  $\varepsilon''(t)$ . This finding signals that doped cubic ice displays enhanced dielectric dynamics that is

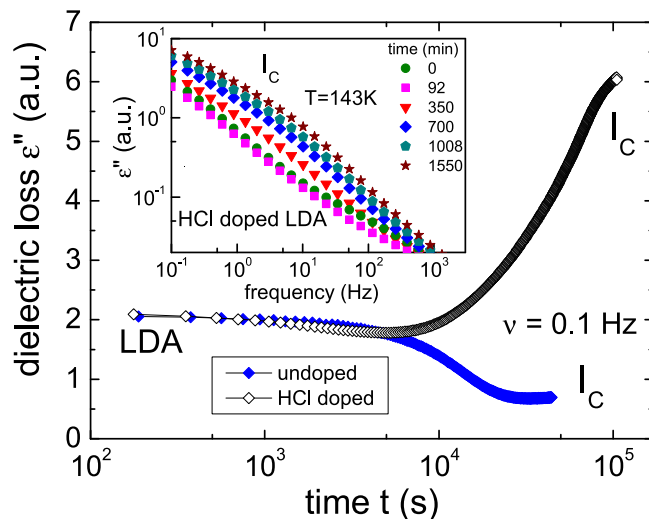


FIG. 4. Time dependence of the dielectric loss measured at 143 K as the transformation of LDA to cubic ice progresses. Doped LDA (black open diamonds) and undoped LDA (blue filled diamonds) show opposite behavior. This finding is compatible with the expectation that in the undoped cubic ice (in the figure marked by  $I_C$ ), little hydrogen atom dynamics occurs, while in the doped material, the large loss reflects significant dynamics. The inset shows several dielectric loss spectra of the HCl doped sample as measured at various annealing times.

analogously known to occur for a number of other suitably doped crystalline ice phases.<sup>42,43</sup>

For doped and undoped amorphous samples, very similar dielectric losses are initially observed, but for the undoped specimen, a loss reduction emerges in the course of crystallization. Thus, as revealed by the two  $\varepsilon''(t)$  curves in Fig. 4, for the undoped material, the dynamics of cubic ice is slower than that of LDA while for the doped crystals it is faster. However, for LDA, the dielectric loss is essentially insensitive to doping which suggests that LDA's microscopic dynamics is not affected by HCl, neither its structural relaxation nor its transformation.

## B. High-pressure volumetry

In order to study the effects of pressure on the HDA to LDA transformation times, we produced HDA samples in our piston-cylinder apparatus and observed the volume changes upon isobaric heating dilatometrically. Figure 5(a) shows the volume changes occurring upon heating HDA at 1 and 4 MPa. The curve recorded at 4 MPa shows a rapid volume increase in the 130–140 K range. The minor linear changes before and after the rapid increase due to thermal expansion of HDA and LDA, respectively, were subtracted in Fig. 5(a). In order to understand the evolution of the dilatometric curve, we performed powder x-ray diffraction using  $\text{Cu K}\alpha$  radiation ( $\lambda = 1.541 \text{ \AA}$ ) on quench-recovered samples of initial HDA, final LDA, and an intermediate state (obtained from HDA heated to  $\sim 139 \text{ K}$ ). The diffractograms presented along the volumetric 4 MPa curve show broad halo-peaks, but no sharp Bragg peaks, see Fig. 5(b), with the exception of the peaks associated with the sample holder (made of nickel-plated copper).

The volumetric 4 MPa curve shown in Fig. 5(a) corresponds to a transition from one amorphous state to another, associated with a  $\approx 25\%$  volume change. Specifically, the halo

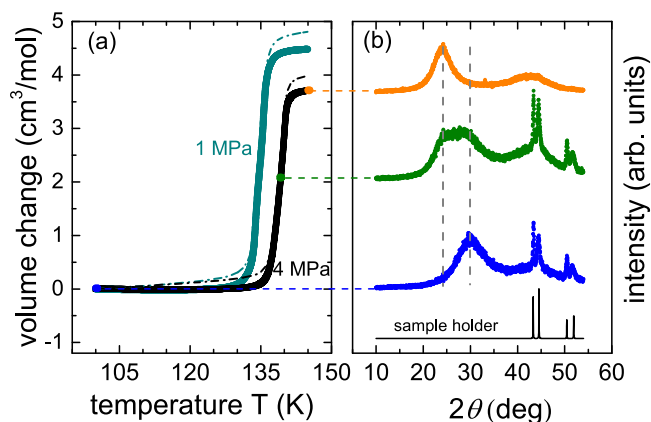


FIG. 5. Initial, intermediate, and final states of the HDA  $\rightarrow$  LDA transition at 1 and 4 MPa. Panel (a) shows the volume change of the complete transition. The raw data are represented by dashed-dotted lines. The thick lines were corrected for thermal expansion effects mainly arising from the amorphous ices. The colored points mark temperatures at which the samples were quenched and recovered to ambient pressure. The corresponding diffractograms recorded after quench-recovery are shown in panel (b). The dotted grey line at  $24.0^\circ$  marks the position of the first diffraction maximum for LDA according to Refs. 44 and 45. The dotted grey line at  $30.0^\circ$  aids seeing shifts in the first diffraction maximum of HDA. The black pattern at the bottom is a calculated diffraction pattern of the sample holder. It should be noted that the difference in the overall volume change seen in panel (a) is not only due to the difference in pressure but also due to the use of a slightly denser HDA starting material that was decompressed to 200 MPa (1 MPa curve) rather than to 100 MPa (4 MPa curve), see Sec. II.

peak maximum “jumps” from a scattering angle  $2\theta$  of about  $30^\circ$  at 80 K characteristic of HDA to about  $24^\circ$  at 150 K characteristic of LDA. The diffractogram recorded for the sample recovered near 139 K can be explained as a linear combination of the LDA and HDA patterns. This finding implies macroscopic separation between the two amorphous ices and the growth of LDA domains within HDA not only for isothermal transitions of samples pressurized to the GPa range<sup>18,39</sup> but also for isobaric transitions of samples close to ambient pressure. Similar observations were also made for pressures of 1 MPa, see Fig. 5(a), and 2 MPa (not shown): It is evident that the end point of the transformation shifts from about 135 K at 1 MPa to about 140 K at 4 MPa, i.e., increased pressure impedes the transition to LDA.

Although, in Ref. 34, an elaborate method has been suggested to evaluate such volumetric data quantitatively, we refrain from applying this approach here. While the dielectric data shown in Fig. 3 refer to isothermal experiments at time scales of the order of  $10^5$  s at ambient pressure near 120 K, the volumetric experiments involve temperature ramping at rates of 2 or 3 K/min, i.e., time scales of the order of  $10^2$  to  $10^3$  s. The combination of faster experimental time scale and higher pressure obviously shifts the volumetric transformation to higher temperatures. Still, the phenomenology and the sharpness of the transition are strikingly similar to the dielectric results, qualitatively suggesting that indeed the time scale of transformation is probed in the  $\epsilon''(t)$  experiment. However, it would be rather difficult to compare the volumetric transformation time scales reliably with the dielectric ones without invoking more or less justified assumptions or extrapolations.

## IV. DISCUSSION

In view of the arguments just given, in this section we focus on the time scales that can be obtained from the dielectric relaxation and transformation experiments. Regarding the latter, it is noted that the behavior evident from Fig. 3 is reminiscent of time evolutions characterizing typical first-order phase transformations. Such transformations are often describable by an Avrami function,

$$\epsilon''(t) \propto \exp[-(t/\tau_{\text{trans}})^\alpha]. \quad (1)$$

Here  $\tau_{\text{trans}}$  designates a transformation time and  $\alpha = 2-4$  is an exponent which depends on the nucleation rate and dimensionality of the growth process. In fact, in analyses of neutron scattering experiments,<sup>27,28</sup> Eq. (1) was used to describe the transformation from uHDA to LDA and exponents in the range  $\alpha = 3.5-4$  were noted.<sup>27</sup> We also attempted to parameterize the data shown in Fig. 3 in terms of Eq. (1). However, the fitting achieved using this approach is far from satisfactory. This is because (i) the initial stages of the transformation cannot be described using Eq. (1) and (ii) even if the time range for the fit is arbitrarily chosen, the exponents are larger than 4 (in some cases up to  $\alpha = 5$ ). Thus, the shapes of the transformation curves are hard to evaluate quantitatively. This precludes statements concerning the dimensionality of the growth process. More importantly, the time scales associated with the rather abrupt HDA  $\rightarrow$  LDA transformations can be determined easily, e.g., from the  $1/e$  decay times of the steep curves shown in Fig. 3.

Before discussing the temperature dependences of the various time scales, Fig. 3 allows for several interesting observations: In light of the strong deuteration induced slow-down that was detected for the structural relaxation, see Fig. 1, a similar isotope effect may have been expected for the transformation kinetics as well. However, when comparing data taken at the same temperature, see Fig. 3, one observes that the deuterated samples transform even slightly (less than a factor of 2 though) faster than their protonated counterparts. Obviously, structural relaxation on the one hand and transformation kinetics on the other are governed by different physical mechanisms.

Figure 3(b) features transformation data acquired using HCl as well as for KOH doped samples. Comparison with the results for an undoped specimen reveals that these dopants are unable to alter the LDA growth rate in any appreciable manner. It is tempting to associate this finding with the insensitivity of the dielectric dynamics reported on the basis of high-pressure (1 GPa) studies that yielded very similar time scales for pure and for KOH doped high-density amorphous ices.<sup>15,16</sup> However, in view of the just made conjecture that relaxation and transformation mechanisms may be different, caution is warranted when comparing the two phenomena directly. Merely, it appears that the transformation of the amorphous ice network — better: amorphous oxygen network — is hardly affected by changes taking place on the hydrogen subsystem.

To put the time scales for the various amorphous ices in perspective, in Fig. 6 we compile the dielectric results obtained for the transformation kinetics and for the structural relaxation times. The structural relaxation times show a large

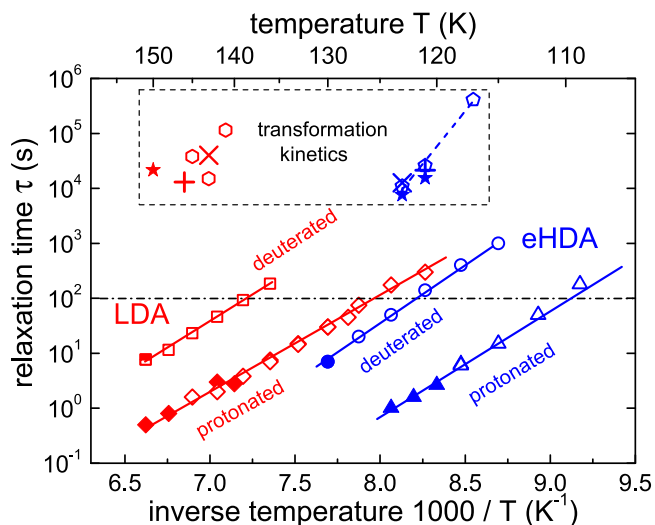


FIG. 6. Arrhenius plot of time scales from ambient-pressure dielectric spectroscopy. First focusing on the structural relaxation times, the triangles refer to protonated HDA, the circles refer to deuterated HDA, the diamonds refer to protonated LDA, and the squares refer to deuterated LDA. The filled symbols correspond to time constants obtained directly from the susceptibility maxima; the open symbols are obtained via frequency-temperature superposition, see Ref. 48. The half-filled point for deuterated LDA was obtained by matching the high-frequency flank of the main process to that of the protonated sample. The solid lines are calculated using Eq. (2). The black dashed-dotted line marks a relaxation time of 100 s. The data in the box represent transformation time scales. Here, the open symbols correspond to protonated, and filled stars refer to deuterated ices; pluses and crosses refer to protonated HCl and KOH doped ice samples, respectively. The dashed blue line that parameterizes the HDA → LDA transformation time scales corresponds to an activation energy of 74 kJ/mol. For the LDA → cubic ice transformation, a description in terms of an Arrhenius law is not indicated on the basis of the present data. The structural relaxation times for protonated HDA and LDA are taken from Ref. 14 and those for deuterated LDA from Ref. 29, all other data are from the present work.

H/D isotope effect for LDA as well as for HDA. As seen in Fig. 6 they obey an Arrhenius law

$$\tau = \tau_0 \exp(E/RT) \quad (2)$$

to a good approximation. Here  $\tau_0$  is a pre-exponential factor,  $E$  denotes an activation energy, and  $R$  is the ideal gas constant. From Fig. 6 one recognizes that the energies are all of a similar magnitude, ranging from 34 kJ/mol for protonated LDA to 42 kJ/mol for deuterated HDA. As pointed out in Sec. III A, the isotope effect for HDA is even larger than it is for LDA, suggesting that also here quantum effects might be at stake.<sup>46</sup> For HDA-H<sub>2</sub>O, the glass transition temperature evaluated as the temperature at which the dielectric relaxation time is 100 s is  $T_g \approx 110$  K.<sup>14</sup> For HDA-D<sub>2</sub>O, the dielectric  $T_g$  shifts by 12 K to 122 K. This is slightly higher than the calorimetric  $T_g$  of HDA-D<sub>2</sub>O of  $118 \pm 1$  K that was determined by Shephard and Salzmann at a heating rate of 10 K/min.<sup>47</sup> When comparing these  $T_g$  values, one should keep in mind that the preparation histories of the amorphous ices are slightly different. While the present samples are obtained by decompressing to 0.1 GPa, cf. Sec. II, decompressing to 0.3 GPa was used in Ref. 47. We furthermore note that the isotope effect on HDA's glass transition temperature is larger in the dielectric experiment than the isotope effect obtained by comparing the calorimetric glass transition temperatures for HDA in Refs. 14 and 47. A similar observation was made previously for LDA and explained on

the basis of a heating-rate dependent isotope effect on  $T_g$  (see Fig. 2G in Ref. 29).

The time scale it takes at ambient pressure for HDA to transform to the low-density state is similar for H<sub>2</sub>O- and D<sub>2</sub>O-samples (see Fig. 6). In view of the absence of a pronounced isotope effect with respect to  $\tau_{\text{trans}}$ , it is clear that the time scale separation of structural relaxation and transformation kinetics is much larger for the protonated than it is for the deuterated sample. Nevertheless, also for the latter, this time scale decoupling amounts to at least three orders of magnitude. Thus, although it is clear that HDA and LDA represent non-equilibrium states, they are sufficiently (meta-)stable so that it is possible to explore many of their properties in an experimentally well-defined manner.

It is interesting to observe that the structural relaxation times are much shorter than the transformation times and that the latter display a more pronounced temperature dependence than the former. However, the transformation times  $\tau_{\text{trans}}$  were not accessible in a sufficiently wide range to allow for a critical test of whether or not  $\tau_{\text{trans}}$  really follows thermally activated behavior, cf. Eq. (2). Nevertheless, the  $\tau_{\text{trans}}(T)$  dependence is compatible with this expression, and for the HDA → LDA transformation, an effective activation energy of about  $74 \pm 5$  kJ/mol is found. Regarding the LDA → cubic ice transformation, a well-defined temperature dependence is not discernible.

Regarding the structural relaxation times, there is a large H/D isotope effect for LDA<sup>29</sup> and HDA, see Fig. 6, and also for amorphous solid water.<sup>13</sup> Recently, in addition, oxygen isotope substitution effects were explored for LDA and HDA.<sup>47</sup> Interestingly, calorimetric experiments of ices produced from H<sub>2</sub><sup>18</sup>O yielded the same glass transition temperatures as the H<sub>2</sub>O samples, in contrast to what can be observed when comparing H<sub>2</sub>O with D<sub>2</sub>O specimens.<sup>47</sup> The findings in Ref. 47 were interpreted in terms of a two-stage scenario to show that the observed glass transition is governed by reorientational motions of the water molecules and that possible translational motion could set in at a higher temperature.<sup>47</sup> Information regarding a possible isotope effect on the transformation kinetics of <sup>18</sup>O enriched amorphous ice samples is not available. In view of the missing H/D isotope effect of  $\tau_{\text{trans}}$ , an <sup>18</sup>O isotope effect regarding this quantity is not necessarily expected. Related experimental tests are, however, beyond the scope of the present work, and so we do not advance any inferences concerning the question whether translational and/or rotational motion of the water molecules is involved in the dynamics of HDA and LDA above their glass transition temperatures. However, based on the data in Fig. 6, we can state that at temperatures above 125 K (protonated samples) and 139 K (deuterated samples), the relaxation time is shorter than 100 s for both high- and low-density samples. That is, if translational motion of water molecules is contributing to the dielectric relaxation, a transition between two ultraviscous liquids (from high-density to low-density liquid) is expected to occur at ambient pressure. In any case, the transformation kinetics do not display an H/D isotope effect, see Fig. 6, a finding suggesting that this process involves the restructuring of the amorphous ices' oxygen rather than just their hydrogen networks.

## V. CONCLUSIONS

In the present article, we report dielectric spectra of deuterated HDA above its glass transition temperature and compare them with spectra of the protonated analogs. The dielectric relaxation times are found to show an even more pronounced H/D isotope effect than the one previously demonstrated for LDA. The HDA  $\rightarrow$  LDA transformation kinetics was monitored for several temperatures and turned out to proceed considerably slower than the dielectric relaxation. That is, there is a separation of transformation and relaxation time scales of at least 3 orders of magnitude. From this perspective, HDA can be regarded as a metastable rather than an instable, ill-defined material, even at ambient pressure. Similar observations were made for the dielectric relaxation in LDA and for the LDA  $\rightarrow$  cubic ice transformation. Thus, from an experimentalist's viewpoint, near their glass transition temperatures, the amorphous ices are well defined on the time scale set by the reorientational motion of the water molecules. We found that the transformation times are not significantly affected by HCl or KOH doping, and also an H/D isotope effect on the polyamorphic transition is not discernible in the present data, in accord with expectations for a restructuring of the amorphous oxygen networks. An increase of pressure, however, impedes the transformation. Furthermore, we understand the changes in the dielectric loss that occur upon heating to imply macroscopic phase separation rather than homogeneous mixing on the molecular scale.

## ACKNOWLEDGMENTS

We thank the Deutsche Forschungsgemeinschaft, Grant No. BO1301/12-1, and the Austrian Science Fund FWF, bilateral Project No. I1392 to T.L. and Erwin Schrödinger Fellowship No. J3811 N34 to P.H.H., for the financial support of this project. V.F.L. is a recipient of a DOC fellowship of the Austrian Academy of Sciences ÖAW.

<sup>1</sup>O. Mishima, L. D. Calvert, and E. Whalley, "An apparently first-order transition between two amorphous phases of ice induced by pressure," *Nature* **314**, 76 (1985).

<sup>2</sup>The term polyamorphism was coined for another tetrahedral liquid in the work by G. H. Wolf, S. Wang, C. A. Herbst, D. J. Durben, W. F. Oliver, Z. C. Kang, and K. Halvorson, "Pressure induced collapse of the tetrahedral framework in crystalline and amorphous GeO<sub>2</sub>," in *High-Pressure Research: Application to Earth and Planetary Sciences*, edited by Y. Syono and M. H. Manghnani (American Geophysical Union, Washington, DC, 1992), p. 503.

<sup>3</sup>P. H. Poole, T. Grande, C. A. Angell, and P. F. McMillan, "Polyamorphic phase transitions in liquids and glasses," *Science* **275**, 322 (1997); P. H. Poole, T. Grande, F. Sciortino, H. E. Stanley, and C. A. Angell, "Amorphous polymorphism," *Comput. Mater. Sci.* **4**, 373 (1995).

<sup>4</sup>J. C. Palmer, F. Martelli, Y. Liu, R. Car, A. Z. Panagiotopoulos, and P. G. Debenedetti, "Metastable liquid-liquid transition in a molecular model of water," *Nature* **510**, 385 (2014).

<sup>5</sup>K. Amann-Winkel, R. Böhmer, C. Gainaru, F. Fujara, B. Geil, and T. Loerting, "Colloquium: Water's controversial glass transitions," *Rev. Mod. Phys.* **88**, 011002 (2016).

<sup>6</sup>O. Mishima, "Reversible first-order transition between two H<sub>2</sub>O amorphs at  $\sim$ 0.2 GPa and  $\sim$ 135 K," *J. Chem. Phys.* **100**, 5910 (1994).

<sup>7</sup>O. V. Stal'gorova, E. L. Gromnitskaya, V. V. Brazhkin, and A. G. Lyapin, "Mechanism and kinetics of the reversible transformation *lda-hda* of amorphous ice under pressure," *JETP Lett.* **69**, 694 (1999).

<sup>8</sup>E. L. Gromnitskaya, O. V. Stal'gorova, A. G. Lyapin, V. V. Brazhkin, and O. B. Tarutin, "Elastic properties of D<sub>2</sub>O ices in solid-state amorphization and transformations between amorphous phases," *JETP Lett.* **78**, 488 (2003).

<sup>9</sup>E. L. Gromnitskaya, I. V. Danilov, A. G. Lyapin, and V. V. Brazhkin, "Influence of isotopic disorder on solid state amorphization and polyamorphism in solid H<sub>2</sub>O–D<sub>2</sub>O solutions," *Phys. Rev. B* **92**, 134104 (2015).

<sup>10</sup>J. J. Shephard, J. S. O. Evans, and C. G. Salzmann, "Structural relaxation of low-density amorphous ice upon thermal annealing," *J. Phys. Chem. Lett.* **4**, 3672 (2013).

<sup>11</sup>For the theoretical side, see, e.g., Ref. 4 and D. T. Limmer and D. Chandler, "Theory of amorphous ices," *Proc. Natl. Acad. Sci. U. S. A.* **111**, 9413 (2014); F. Smallegange and F. Sciortino, "Tuning the liquid-liquid transition by modulating the hydrogen-bond angular flexibility in a model for water," *Phys. Rev. Lett.* **115**, 015701 (2015); For the experimental side, see, e.g., Sec. III.E in T. Loerting, V. V. Brazhkin, and T. Morishita, *Adv. Chem. Phys.* **143**, 29 (2009).

<sup>12</sup>G. P. Johari, "State of water at 136 K determined by its relaxation time," *Phys. Chem. Chem. Phys.* **7**, 1091 (2005); G. P. Johari, "Dielectric relaxation time of bulk water at 136–140 K, background loss and crystallization effects," *J. Chem. Phys.* **122**, 144508 (2005).

<sup>13</sup>A. L. Agapov, A. I. Kolesnikov, V. N. Novikov, R. Richert, and A. P. Sokolov, "Quantum effects in the dynamics of deeply supercooled water," *Phys. Rev. E* **91**, 022312 (2015).

<sup>14</sup>K. Amann-Winkel, C. Gainaru, P. H. Handle, M. Seidl, H. Nelson, R. Böhmer, and T. Loerting, "Water's second glass transition," *Proc. Natl. Acad. Sci. U. S. A.* **44**, 17720 (2013).

<sup>15</sup>O. Andersson and A. Inaba, "Dielectric properties of high-density amorphous ice under pressure," *Phys. Rev. B* **74**, 184201 (2006).

<sup>16</sup>O. Andersson, "Dielectric relaxation of the amorphous ices," *J. Phys.: Condens. Matter* **20**, 244115 (2008).

<sup>17</sup>R. J. Nelmes, J. S. Loveday, T. Straessle, C. L. Bull, M. Guthrie, G. Hamel, and S. Klotz, "Annealed high-density amorphous ice under pressure," *Nat. Phys.* **2**, 414 (2006).

<sup>18</sup>K. Winkel, E. Mayer, and T. Loerting, "Equilibrated high-density amorphous ice and its first-order transition to the low-density form," *J. Phys. Chem. B* **115**, 14141 (2011).

<sup>19</sup>O. Mishima, L. D. Calvert, and E. Whalley, "'Melting ice' I at 77 K and 10 kbar: A new method of making amorphous solids," *Nature* **310**, 393 (1984).

<sup>20</sup>J. S. Tse, D. D. Klug, C. A. Tulk, I. Swainson, E. C. Svensson, C.-K. Loong, V. Shpakov, V. R. Belosludov, R. V. Belosludov, and Y. Kawazoe, "The mechanisms for pressure-induced amorphization of ice I<sub>h</sub>," *Nature* **400**, 647 (1999).

<sup>21</sup>M. Seidl, K. Amann-Winkel, P. H. Handle, G. Zifferer, and T. Loerting, "From parallel to single crystallization kinetics in high-density amorphous ice," *Phys. Rev. B* **88**, 174105 (2013).

<sup>22</sup>M. Seidl, A. Fayter, J. N. Stern, G. Zifferer, and T. Loerting, "Shrinking water's no man's land by lifting its low-temperature boundary," *Phys. Rev. B* **91**, 144201 (2015).

<sup>23</sup>T. Loerting, C. Salzmann, I. Kohl, E. Mayer, and A. Hallbrucker, "A second distinct structural 'state' of high-density amorphous ice at 77 K and 1 bar," *Phys. Chem. Chem. Phys.* **3**, 5355 (2001).

<sup>24</sup>K. Winkel, M. S. Elsaesser, E. Mayer, and T. Loerting, "Water polyamorphism: Reversibility and (dis)continuity," *J. Chem. Phys.* **128**, 044510 (2008).

<sup>25</sup>J. Stern and T. Loerting, "Crystallisation of the amorphous ices in the intermediate pressure regime," *Sci. Rep.* **7**, 3995 (2017).

<sup>26</sup>H. Schober, A. Tölle, M. Koza, F. Fujara, C. A. Angell, and R. Böhmer, "Amorphous polymorphism in ice investigated by inelastic neutron scattering," *Physica B* **241-243**, 897 (1998).

<sup>27</sup>M. M. Koza, H. Schober, H. E. Fischer, T. Hansen, and F. Fujara, "Kinetics of the high- to low-density amorphous water transition," *J. Phys.: Condens. Matter* **15**, 321 (2003).

<sup>28</sup>M. M. Koza, T. Hansen, R. P. May, and H. Schober, "Link between the diversity, heterogeneity and kinetic properties of amorphous ice structures," *J. Non-Cryst. Solids* **352**, 4988 (2006).

<sup>29</sup>C. Gainaru, A. L. Agapov, V. Fuentes-Landete, K. Amann-Winkel, H. Nelson, K. W. Köster, A. I. Kolesnikov, V. N. Novikov, R. Richert, R. Böhmer, T. Loerting, and A. P. Sokolov, "Anomalously large isotope effect in the glass transition of water," *Proc. Natl. Acad. Sci. U. S. A.* **111**, 17402 (2014).



- <sup>30</sup>W. F. Kuhs, C. Sippel, A. Falenty, and T. C. Hansen, "Extent and relevance of stacking disorder in 'ice Ic,'" *Proc. Natl. Acad. Sci. U. S. A.* **109**, 21259 (2012).
- <sup>31</sup>T. L. Malkin, B. J. Murray, C. G. Salzmann, V. Molinero, S. J. Pickering, and T. F. Whale, "Stacking disorder in ice I," *Phys. Chem. Chem. Phys.* **17**, 60 (2015).
- <sup>32</sup>M. S. Elsaesser, K. Winkel, E. Mayer, and T. Loerting, "Reversibility and isotope effect of the calorimetric glass  $\rightarrow$  liquid transition of low-density amorphous ice," *Phys. Chem. Chem. Phys.* **12**, 708 (2010).
- <sup>33</sup>In particular the crystallization temperature and the associated transformation kinetics depend on the preparation of the samples as well, see Refs. [21](#) and [22](#).
- <sup>34</sup>P. H. Handle and T. Loerting, "Temperature induced amorphisation of hexagonal ice," *Phys. Chem. Chem. Phys.* **17**, 5403 (2015).
- <sup>35</sup>P. H. Handle and T. Loerting, "Dynamics anomaly in high-density amorphous ice between 0.7 and 1.1 GPa," *Phys. Rev. B* **93**, 064204 (2016).
- <sup>36</sup>G. P. Johari, A. Hallbrucker, and E. Mayer, "The dielectric behavior of vapor-deposited amorphous solid water and of its crystalline form," *J. Chem. Phys.* **95**, 2955 (1991); Dielectric study of the structure of hyperquenched glassy water and its crystallized forms," **97**, 5851 (1992).
- <sup>37</sup>P. Lunkenheimer, R. Wehn, U. Schneider, and A. Loidl, "Glassy aging dynamics," *Phys. Rev. Lett.* **95**, 055702 (2005).
- <sup>38</sup>T. Hecksher, N. B. Olsen, K. Niss, and J. C. Dyre, "Physical aging of molecular glasses studied by a device allowing for rapid thermal equilibration," *J. Chem. Phys.* **133**, 174514 (2010).
- <sup>39</sup>S. Klotz, T. Strässle, R. J. Nelmes, J. S. Loveday, G. Hamel, G. Rousse, B. Canny, J. C. Chervin, and A. M. Saitta, "Nature of the polyamorphic transition in ice under pressure," *Phys. Rev. Lett.* **94**, 025506 (2005).
- <sup>40</sup>S. R. Gough and D. W. Davidson, "Dielectric behavior of cubic and hexagonal ices at low temperatures," *J. Chem. Phys.* **52**, 5442 (1970).
- <sup>41</sup>O. Yamamuro, M. Oguni, T. Matsuo, and H. Suga, "Heat capacity and glass transition of pure and doped cubic ices," *J. Phys. Chem. Solids* **48**, 935 (1987).
- <sup>42</sup>V. F. Petrenko and R. W. Whitworth, *Physics of Ice* (University Press, Oxford, 1999).
- <sup>43</sup>For a recent study containing further references, see K. W. Köster, A. Raidt, C. Gainaru, V. Fuentes-Landete, T. Loerting, and R. Böhmer, "Doping-enhanced dipolar dynamics in ice V as a precursor of proton ordering in ice XIII," *Phys. Rev. B* **94**, 184306 (2016).
- <sup>44</sup>A. Bizid, L. Bosio, A. Defrain, and M. Oumezzine, "Structure of high-density amorphous water. I. X-ray diffraction study," *J. Chem. Phys.* **87**, 2225 (1987).
- <sup>45</sup>K. Winkel, D. T. Bowron, T. Loerting, E. Mayer, and J. L. Finney, "Relaxation effects in low density amorphous ice: Two distinct structural states observed by neutron diffraction," *J. Chem. Phys.* **130**, 204502 (2009).
- <sup>46</sup>V. N. Novikov and A. P. Sokolov, "Role of quantum effects in the glass transition," *Phys. Rev. Lett.* **110**, 065701 (2013).
- <sup>47</sup>J. J. Shephard and C. G. Salzmann, "Molecular reorientation dynamics govern the glass transitions of the amorphous ices," *J. Phys. Chem. Lett.* **7**, 2281 (2016).
- <sup>48</sup>An example of this procedure with an application to eHDA is given in Fig. 6 of J. Stern, M. Seidl, C. Gainaru, V. Fuentes-Landete, K. Amann-Winkel, P. H. Handle, K. W. Köster, H. Nelson, R. Böhmer, and T. Loerting, "Experimental evidence for two distinct deeply supercooled liquid states of water—Response to 'Comment on 'Water's second glass transition,'" by G. P. Johari, *Thermochem. Acta* (2015)," *Thermochem. Acta* **617**, 200 (2015).